Schematic phase diagram and collective excitations in the collisional regime for trapped boson-fermion mixtures at zero temperature

A. Minguzzi [a,1] and M. P. Tosi [a]

[a] *Istituto Nazionale di Fisica della Materia and Classe di Scienze, Scuola Normale Superiore, Piazza dei Cavalieri 7, I-56126 Pisa, Italy*

Abstract

We discuss the ground state and the small-amplitude excitations of dilute boson-fermion mixtures confined in spherical harmonic traps at $T = 0$, assuming repulsive boson-boson interactions and with each component being in a single hyperfine state. From previous studies of the equilibrium density profiles we propose a schematic phase diagram in a plane defined by the variables a_{bf}/a_{bb} and $a_{bb}k_f^{(0)}$, where a_{bb} and a_{bf} are the boson-boson and boson-fermion scattering lengths and $k_f^{(0)}$ is the Fermi wave number at the centre of the trap. With this background we turn to the equations of motion for density fluctuations in the collisional regime and discuss some general features of the eigenmodes. We display analytic solutions for sound waves in a quasi-homogeneous mixture and for surface modes at weak fermion-boson coupling.

PACS: 03.75.Fi, 05.30.Jp, 67.40.Db

1 Introduction

The achievement of Bose-Einstein condensation in trapped atomic gases [1 - 3] has given new impulse to the study of dilute quantal fluids. Experimental attention has extended to the properties of double Bose condensates [4, 5] and more recently to the attainment of quantal degeneracy in gases of fermionic atoms [6 - 10] and in dilute mixtures of bosons and fermions [11]. A specific

---

[1] Corresponding author. Tel.: +39 50 509058; fax: +39 50 563513; e-mail: minguzzi@cibs.sns.it.

motivation for interest in boson-fermion mixtures is that the collisions between fermions and bosons can foster thermalization of the fermionic component and induce so-called sympathetic cooling [4, 12]. Elastic collisions between fermions in a single hyperfine state are inhibited by the Pauli principle [13] and even in multi-component Fermi gases the collisions between atoms in different hyperfine states become ineffective at very low temperature because of Fermi factors [9].

A number of theoretical studies have already been addressed to properties of dilute boson-fermion mixtures confined in harmonic traps. They have concerned the equilibrium density profiles of the two species both at zero and at finite temperature [14 - 17], the kinetic energy of the fermionic component [18] and collective excitations from sum rules in the collisionless regime [19]. Our main focus here is on small-amplitude collective excitations for a mixture under harmonic confinement in the collisional regime. For a detailed discussion on how this regime may be achieved in dilute Fermi gases we refer to the work of Amoruso *et al.* [20].

We first set up a general background for our discussion of collective excitations in boson-fermion mixtures by constructing a schematic phase diagram from the earlier studies of the equilibrium state [14 - 18]. This helps to identify various dynamical behaviours, which may later be examined in detail by explicit numerical solution of the equations of motion. We then report analytic results for the eigenfrequencies of the mixture in limiting situations, corresponding to mixing of Bogolubov sound and fermionic first sound in a nearly homogeneous mixture and to surface modes in a regime of weak fermion-boson coupling.

We assume throughout a positive boson-boson scattering length, as is applicable to Bose condensates of ^{87}Rb and ^{23}Na. Mixtures of ^{6}Li and ^{7}Li should have special interest, once condensation is realized for ^{7}Li in a hyperfine state where the scattering length is positive. According to calculations on the collisional properties of ultracold potassium [21], the ^{40}K-^{41}K mixture should also be an interesting system for study from the present viewpoint, if condensation of the rare isotope ^{41}K can be achieved.

2 Equilibrium density profiles and phase diagram

We consider a system of N_f fermions of mass m_f and N_b bosons of mass m_b at $T = 0$, confined by spherically symmetric external potentials $V_{f,b}(r) = m_{f,b}\omega_{f,b}^2 r^2/2$ with frequencies ω_f and ω_b. We assume that a single spin state is trapped for each component of the mixture and that all bosons are in the condensate. We can then omit the fermion-fermion interaction, which is inhibited by the Pauli exclusion principle. The boson-boson and boson-fermion inter-

actions are described by contact potentials with scattering lengths $a_{bb} > 0$ and a_{bf}, yielding coupling-strength parameters $g = 4\pi\hbar^2 a_{bb}/m_b > 0$ and $f = 2\pi\hbar^2 a_{bf}/m_r$ where m_r is the reduced boson-fermion mass.

The equations of motion for the partial particle densities $n_\sigma(\mathbf{r}, t)$ and partial current densities $\mathbf{j}_\sigma(\mathbf{r}, t)$, where σ is an index for the atomic species ($\sigma = f$ or b) follow from those for the one-body density matrix upon projection on the main diagonal (see for instance [22]). They take the form of continuity equations,

$$\partial_t n_\sigma(\mathbf{r}, t) = -\nabla \cdot \mathbf{j}_\sigma(\mathbf{r}, t) \tag{2.1}$$

and of generalized hydrodynamic equations which, in a mean-field approximation and neglecting coupling to energy fluctuations, can be written as

$$m_f \partial_t \mathbf{j}_f(\mathbf{r}, t) = -\nabla \cdot \Pi^{(f)}(\mathbf{r}, t) - n_f(\mathbf{r}, t)\nabla\left[V_f(\mathbf{r}) + f n_b(\mathbf{r}, t) - \mu_f\right] \tag{2.2}$$

and

$$\begin{aligned} m_b \partial_t \mathbf{j}_b(\mathbf{r}, t) = &-\nabla \cdot \Pi^{(b)}(\mathbf{r}, t) \\ &- n_b(\mathbf{r}, t)\nabla\left[V_b(\mathbf{r}) + g n_b(\mathbf{r}, t) + f n_f(\mathbf{r}, t) - \mu_b\right] \end{aligned} \tag{2.3}$$

In these equations $\Pi^{(\sigma)}(\mathbf{r}, t)$ are the kinetic stress tensors and μ_σ are the chemical potentials of the two atomic species. In the following we treat the kinetic stress tensors by a local density approximation for fermions,

$$\Pi^{(f)}_{ij}(\mathbf{r}, t) = \frac{2}{5}A[n_f(\mathbf{r}, t)]^{5/3}\delta_{ij} \tag{2.4}$$

with $A = \hbar^2(6\pi^2)^{2/3}/2m_f$ and by a Thomas-Fermi approximation for bosons,

$$\Pi^{(b)}(\mathbf{r}, t) = 0 . \tag{2.5}$$

In these equations we have dropped terms which are quadratic in the velocity field.

The treatment given above assumes that local equilibrium has been established for the ground-state density profiles and that it is maintained during dynamic fluctuations of the particle densities. The dynamical behaviour that we shall discuss in Sect.3 will therefore correspond to a collisional regime [20].

2.1 Equilibrium density profiles

The equilibrium density profiles ($n_\sigma^{eq}(r)$, say) follow from Eqs. (2.2) - (2.5) by setting the current densities to zero. The results are well known [14, 15]:

$$n_b^{eq}(r) = g^{-1}\left[\mu_b - V_b(r) - fn_f^{eq}(r)\right]\theta(\mu_b - V_b(r) - fn_f^{eq}(r)) \qquad (2.6)$$

and

$$n_f^{eq}(r) = A^{-3/2}\left[\mu_f - V_f(r) - fn_b^{eq}(r)\right]^{3/2}\theta(\mu_f - V_f(r) - fn_b^{eq}(r)) . \quad (2.7)$$

The chemical potentials are to be determined by self-consistency conditions on the particles numbers, $N_\sigma = \int n_\sigma^{eq}(r)d\mathbf{r}$. On comparing the two density profiles in the limit of vanishing boson-fermion coupling, it is easily seen that the quantity $(2A/3)[n_f^{eq}(r)]^{-1/3}$ may be viewed as an effective fermion-fermion coupling arising from the kinetic pressure of the Fermi gas [23]. It is also useful to introduce the radii $R_b = (2\mu_b/m_b\omega_b^2)^{1/2}$ and $R_f = (2\mu_f/m_f\omega_f^2)^{1/2}$ for the two clouds in the absence of interactions, but taken at the true values of the chemical potentials.

For values of the boson-boson coupling and of the confinement frequencies which are typical of current experiments, and assuming comparable magnitudes for the boson-boson and the boson-fermion coupling, the fermionic cloud is considerably more dilute than the bosonic cloud. In this situation the boson cloud is essentially unaffected by the interactions with the fermionic component and the latter can be treated as confined inside a double-parabola effective potential $V_f^{eff}(r)$ [15]. This is given by

$$V_f^{eff}(r) = \begin{cases} m_f\omega_f^2(1-\gamma)r^2/2 + f\mu_b/g & \text{for } r < R_b \\ m_f\omega_f^2 r^2/2 & \text{for } r > R_b \end{cases} \qquad (2.8)$$

where

$$\gamma = (fm_b\omega_b^2)/(gm_f\omega_f^2) . \qquad (2.9)$$

Evidently, if $\gamma > 1$ the effective potential (2.8) has negative concavity inside the Bose radius and the fermions will tend to be expelled from the centre of the trap. The result at strong coupling is phase separation in the mixture, with the fermions forming a shell around the boson cloud [15].

A second type of phase separation for the boson-fermion mixture was demonstrated in the work of Mølmer [14]. In this case one takes $N_f \simeq N_b$ and consid-

ers very large values of the boson-boson coupling g, such that the two clouds acquire similar densities. One ultimately finds that the bosons are expelled from the centre of the trap and form a shell around the fermion cloud.

Finally, Eq. (2.8) is valid also in the case $\gamma < 0$, *i.e.* for attractive boson-fermion interactions, as long as the fermionic cloud is more dilute than the boson cloud. However, the fermions now tend to draw the bosons towards the centre of the trap, ultimately leading to collapse once γ becomes sufficiently negative [24].

2.2 Schematic phase diagram at zero temperature

As shown by Vichi *et al.* [18], the thermodynamics of the boson-fermion mixture at $T = 0$ is well characterized by means of two scaling parameters, which are γ in Eq. (2.9) and

$$x = \left(\frac{R_b}{R_f}\right)^{1/2} = \left(\frac{m_f\omega_f}{2m_b\omega_b}\right)^{1/2} \left[15\frac{a_{bb}}{a_{ho}}\frac{N_b}{(6N_f)^{5/6}}\right]^{1/5} , \qquad (2.10)$$

with $a_{ho} = (\hbar/m_b\omega_b)^{1/2}$. The description of the system with only two scaling parameters, instead of the eight original ones entering the expression of the equilibrium density profiles, is a major simplification. The ratio R_b/R_f determines the deviation of the kinetic energy of the fermion cloud from its ideal-gas value [18].

For the purposes of the present discussion we make the simplifying assumptions $m_f = m_b$, $\omega_f = \omega_b$ and $N_f = N_b$. In this case the two scaling parameters take the simple expressions $x = (15a_{bb}k_f^{(0)}/48)^{1/5}$ and $\gamma = a_{bf}/a_{bb}$, with $k_f^{(0)} = (48N_f)^{1/6}/a_{ho}$ being the Fermi wave number at the trap centre for a non-interacting Fermi gas. As remarked under Eq. (2.7) above, the quantity $a_{ff} \equiv 3\pi/4k_f^{(0)}$ may be viewed as an effective fermion-fermion scattering length arising from the Pauli kinetic pressure. We can now proceed to construct a schematic phase diagram for the boson-fermion mixture in the plane defined by the variables $\gamma = a_{bf}/a_{bb}$ and $y = a_{bb}k_f^{(0)}$. Figure 1 shows the result for the case $\gamma > 0$ (*i.e.* repulsive boson-fermion interactions).

We search for the boundary of phase separation by means of a simple condition of linear stability on the two-by-two matrix of scattering lengths a_{bb}, a_{bf} and a_{ff} [23] (see also [25]). A mixed state is stable if the inequality $a_{bb}a_{ff} - a_{bf}^2 > 0$ holds, *i.e.* when

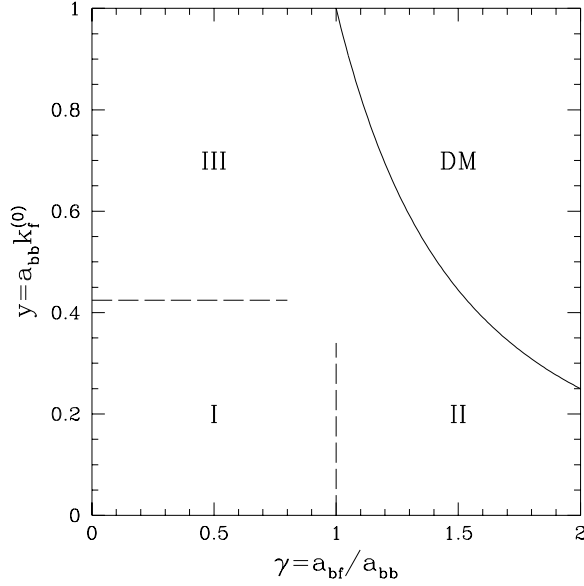$$k_f^{(0)}a_{bb} \leq \frac{3\pi}{4}\left(\frac{a_{bb}}{a_{bf}}\right)^2 \qquad (2.11)$$

Fig. 1. Schematic phase diagram of boson-fermion mixtures in a spherical harmonic trap, for the case of repulsive boson-boson and boson-fermion interactions. The phase-separation region is marked DM (for "demixed"). See the main text for a description of areas I, II and III in the miscibility region.

Within this region we can distinguish a region of appreciable overlap between the two clouds (region I in Figure 1), bounded by two regions of diminishing overlap: a region at $\gamma > 1$ where the fermions are being expelled from the centre of the trap (region II in Figure 1) and by a region at $y > 4/3\pi$ where the bosons are being expelled from the centre of the trap (region III in Figure 1). If the spherical symmetry of the trapping potential is preserved in the demixed state, these two regions end into spherical-shell structures with the fermions at large γ (or the bosons at large y) forming the outer shell.

3   Small amplitude oscillations around the equilibrium profiles

The equations of motion for small-amplitude density fluctuations $\tilde{n}_f(\mathbf{r}, t)$ and $\tilde{n}_b(\mathbf{r}, t)$ in the collisional regime are found by combining Eq. (2.1) with the linearized form of Eqs. (2.2) and (2.3). They are

$$\partial_t^2 \tilde{n}_f(\mathbf{r}, t) = \frac{1}{m_f} \nabla \cdot \left\{ n_f^{eq}(r) \nabla \left[\frac{2}{3} A (n_f^{eq}(r))^{-1/3} \tilde{n}_f(\mathbf{r}, t) + f \tilde{n}_b(\mathbf{r}, t) \right] \right\} \quad (3.1)$$

and

$$\partial_t^2 \tilde{n}_b(\mathbf{r}, t) = \frac{1}{m_b} \nabla \cdot \left\{ n_b^{eq}(r) \nabla \left[g \tilde{n}_b(\mathbf{r}, t) + f \tilde{n}_f(\mathbf{r}, t) \right] \right\} \ . \qquad (3.2)$$

6

Again the quantity $(2A/3)[n_f^{eq}(r)]^{-1/3}$ enters Eq. (3.1) as an effective fermion-fermion coupling.

It is easily checked that the form of Eqs. (3.1) and (3.2) is such as to satisfy the generalized Kohn theorem [26, 27] for the centre-of-mass coordinate $\mathbf{x}(t)$ of the whole fluid when the two confinement frequencies coincide. In this mode of motion we have $n_{b,f}(\mathbf{r},t) = n_{b,f}^{eq}(\mathbf{r}-\mathbf{x}(t))$ and hence

$$\tilde{n}_{b,f}(\mathbf{r},t) = -\mathbf{x}(t) \cdot \nabla n_{b,f}^{eq}(r) \qquad (3.3)$$

for small amplitude oscillations. By substituting Eq. (3.3) in Eqs. (3.1) and (3.2) and using Eqs. (2.6) and (2.7), we find

$$m_{b,f}\partial_t^2 \mathbf{x}(t) \cdot \nabla n_{b,f}^{eq}(r) = \sum_{i,j} x_j(t)\nabla_i \left[n_{b,f}^{eq}(r)\nabla_i\nabla_j V_{b,f}(r) \right] . \qquad (3.4)$$

Therefore, the centre of mass of the system oscillates at the bare trap frequency.

Evidently, a general solution of Eqs. (3.1) and (3.2) can only be obtained numerically, since the equilibrium density profiles are not known analytically from Eqs. (2.6) and (2.7). The dynamics of the fluid as a function of the scaling parameters will be especially rich in the regions of the phase diagram in which the nature of the partial density profiles is changing on the approach to phase separation. Of course, this will be signalled by a softening of the modes associated with concentration fluctuations. Below we restrict ourselves to analytic results which are applicable to special regimes.

3.1   Homogeneous limit

The dynamics of a spatially homogeneous mixture is relevant to the situation in which the density profiles of both components are slowly varying in space, on the length scale set by the mean interparticle distances. Taking the equilibrium densities as constant, it is easily seen from Eqs. (3.1) and (3.2) that the eigenmodes are two sound waves, with linear dispersion relation $\omega_{1,2}(q) = c_{1,2}q$. The sound velocities are given by

$$c_{1,2}^2 = \frac{1}{2}\left[c_b^2 + c_f^2 \pm \sqrt{(c_b^2 - c_f^2)^2 + 4f^2 n_b^{eq} n_f^{eq}/m_b m_f} \right] . \qquad (3.5)$$

In Eq. (3.5) $c_b = (gn_b^{eq}/m_b)^{1/2}$ is the speed of Bogolubov sound and $c_f = [2A(n_f^{eq})^{2/3}/3m_f]^{1/2}$ is that of first sound in a Fermi gas.

This result may be useful in regard to measurements of the speed of sound in elongated systems, in experiments such as already carried out by Matthews *et al.* [30] on a single Bose condensate.

3.2   Surface modes for weak boson-fermion coupling

Assuming equal confinement frequencies for the two components of the mixture (ω_{ho}, say), it is known from earlier results of Stringari [28] for a Bose condensate and of Amoruso *et al.* [29] for a one-component Fermi gas that in the limit $f = 0$ the frequencies of the surface modes ($n = 0$) with angular momentum number are equal and given by $\omega_l = l^{1/2}\omega_{ho}$. A perturbative treatment of the effect of fermion-boson coupling is therefore especially simple for these modes.

We define the unperturbed equilibrium density profiles $n_{b,f}^{(0)}(r)$ and the $\mathbf{r}$-dependent amplitudes $\tilde{n}_{b,f}^{(l,m)}(\mathbf{r})$ of the unperturbed density fluctuations, for each value of the angular momentum l and of its z-component m. After Fourier-transforming Eqs. (3.1) and (3.2) and linearizing them in the coupling parameter f, we multiply Eq. (3.1) by $[n_f^{(0)}(r)]^{-1/3}\tilde{n}_f^{(l,m)}(\mathbf{r})$ and Eq. (3.2) by $\tilde{n}_b^{(l,m)}(\mathbf{r})$, and then integrate both equations over $\mathbf{r}$. We obtain in this way a determinantal equation for the shift of the eigenmode frequencies Ω_l due to the fermion-boson coupling. Writing

$$\Omega_l^2 = \omega_{ho}^2(l + \Delta_l) , \qquad (3.6)$$

we find

$$\Delta_l = \frac{a_{bf}}{2a_{ho}}\left[-(E + B) \pm \text{sign}(a_{bf})\sqrt{(E - B)^2 + 4CD}\right] , \qquad (3.7)$$

this result being valid for either sign of a_{bf}. The quantities entering Eq. (6) are defined in the Appendix, where it is also shown that they can all be expressed in terms of the Gauss hypergeometric function [31].

The result given in Eq. (3.7) should be better applicable in the case $R_b < R_f$, since in deriving it we have assumed that the equilibrium density profiles for both components are perturbed in a symmetric manner. This corresponds to working in region I of the phase diagram (and in the corresponding region at negative γ).

8

4   Summary and discussion

The main features of the zero-temperature phase diagram that we have sketched in Figure 1 for boson-fermion mixtures arise from the competition between the kinetic energy of the Fermi gas and the repulsive boson-boson and boson-fermion interactions. The former disfavours localization and phase separation, while the latter favour the spatial separation of the two components. On varying these system parameters while preserving the spherical symmetry of the trapped fluid mixture, a spontaneous symmetry breaking occurs towards a situation where the two components are spatially separated along the radial direction. Evidently, axial separation of the two components would instead be observed in an anisotropic trap. One may think of exploiting Feshbach resonances to tune the scattering lengths towards such phase-separation regime.

Given the complex behaviour of the density profiles on the approach to phase separation, a complete investigation of the oscillatory eigenmodes of a boson-fermion mixture can only be carried out by numerical means. This will be well worth doing once a mixture of specific experimental relevance and with reasonably known scattering lengths is identified. Of course, the dynamics in the phase-separated region is simply related to that of the two pure components, aside for the presence of interfacial modes. On the other hand, we have seen that suggestive analytic results can be obtained in the quasi-homogeneous limit and in the weak boson-coupling regime, for either sign of the boson-fermion coupling. With increasingly large attractions between boson and fermions, however, the mixture is expected to undergo collapse [24].

A   Calculation of frequency shifts for surface modes

We introduce the notations $|F\rangle = \tilde{n}_f^{(l,m)}(\mathbf{r})$ and $|B\rangle = \tilde{n}_b^{(l,m)}(\mathbf{r})$, define the operators $P_{b,f} = (f/m_{b,f})\nabla\cdot[n_{b,f}^{(0)}(r)\nabla]$ and $D_f = (-f/m_f)\nabla\cdot\{(n_f^{(0)}(r))^{1/3}\nabla[(n_f^{(0)}(r))^{-1/3}]\}$, and introduce the scalar-product notation $\langle F|\hat{O}|F\rangle = \int \tilde{n}_f^{(l,m)}(\mathbf{r})\hat{O}n_f^{(l,m)}(\mathbf{r})d\mathbf{r}$ etcetera. With these notations we find the following expressions for the quantities entering Eq. (3.7):

$$B = \langle F | (n_f^{(0)}(r))^{-1/3} D_f | F \rangle / \langle F | (n_f^{(0)}(r))^{-1/3} | F \rangle$$

$$= \frac{2\pi^{-1/2} l}{\alpha_{bb} X_f^{2l+2}} \frac{\Gamma(l+3)}{\Gamma(l+3/2)} \int_0^{X_b} dx\, x^{2l+2} (X_f^2 - x^2)^{-1/2} (2X_f^2 + X_b^2 - 3x^2), \quad \text{(A.1)}$$

$$C = \langle F | (n_f^{(0)}(r))^{-1/3} P_f | B \rangle / \langle F | (n_f^{(0)}(r))^{-1/3} | F \rangle$$

$$= \frac{-2l}{\pi^{5/2} X_f^{2l+2}} \frac{\Gamma(l+3)}{\Gamma(l+3/2)} \int_0^{X_b} dx\, x^{2l+2} (X_f^2 - x^2)^{1/2}, \quad \text{(A.2)}$$

$$D = \langle B | P_b | F \rangle / \langle B | B \rangle$$

$$= \frac{-(2l+3)}{2\alpha_{bb} X_b^{2l+3}} \int_0^{X_b} dx\, x^{2l+2} \left\{ 2l(X_f^2 - x^2)^{1/2} + X_f^2 (X_f^2 - x^2)^{-3/2} (X_b^2 - x^2) \right.$$

$$\left. + (X_f^2 - x^2)^{-1/2} [-x^2 + 2(l+1)(X_b^2 - x^2)] \right\}, \quad \text{(A.3)}$$

and

$$E = -\langle B | P_f | B \rangle / \langle B | B \rangle$$

$$= \frac{l(2l+3)}{2\pi^2 X_b^{2l+3}} \int_0^{X_b} dx\, x^{2l+2} (X_f^2 - x^2)^{1/2}. \quad \text{(A.4)}$$

In these equations $\Gamma(n)$ is the Gamma function and we have set $X_{b,f} = R_{b,f}/a_{ho}$ and $\alpha_{bb} = a_{bb}/a_{ho}$.

All the integrals in Eqs. (A.1) -(A.4) can be expressed through the Gauss hypergeometric function ${}_2F_1(a, b; c; z)$, using the relation [31]

$$ {}_2F_1\left(\frac{1+\alpha}{2}, -\frac{n}{2}; \frac{3+\alpha}{2}; \frac{X_b^2}{X_f^2} \right) = \frac{1+\alpha}{X_f^n X_b^{\alpha+1}} \int_0^{X_b} dx\, x^\alpha (X_f^2 - x^2)^{n/2}. \quad \text{(A.5)}$$

References

[1] M.H. Anderson, J.R. Ensher, M.R. Matthews, C.E. Wieman, E.A. Cornell, *Science* 269 (1995) 198.

[2] K.B. Davis, M.-O. Mewes, M.R. Andrews, N.J. van Druten, D.S. Durfee, D.M. Kurn, W. Ketterle, *Phys. Rev. Lett.* 75 (1995) 3969.

[3] C.C. Bradley, C.A. Sackett, R.G. Hulet, *Phys. Rev. Lett.* 78 (1997) 985.

[4] C.J. Myatt, E.A. Burt, R.W. Ghrist, E.A. Cornell, C. E. Wieman, *Phys. Rev. Lett.* 78 (1997) 586.

[5] D.S. Hall, M.R. Matthews, J.R. Hensher, C.E. Wieman, E.A. Cornell, *Phys. Rev. Lett.* 81 (1998) 1539.

[6] W.I. McAlexander, E.R.I. Abraham, N.W.M. Ritchie, C.J. Williams, H.T.C. Stoof, R.G. Hulet, *Phys. Rev. A* 51 (1995) R871.

[7] F.S. Cataliotti, E.A. Cornell, C. Fort, M. Inguscio, F. Marin, M. Prevedelli, L. Ricci, G.M. Tino, *Phys. Rev. A* 57, (1998) 1136.

[8] B. DeMarco, J.L. Bohn, J.P. Burke Jr., M. Holland, D.S. Jin, *Phys. Rev. Lett.* 82, (1999) 4208.

[9] B. DeMarco, D.S. Jin, *Science* 285 (1999) 1703.

[10] M.J. Holland, B. DeMarco, D.S. Jin, *cond-mat*/9911017.

[11] M.-O. Mewes, G. Ferrari, F. Schreck, A. Sinatra, C. Salomon, *Phys. Rev. A* 61 (2000) 011403(R).

[12] W. Geist, L. You, T.A.B. Kennedy, *Phys. Rev. A* 59 (1999) 1500.

[13] I. F. Silvera, *Physica B* 109/110 (1982) 1499.

[14] K. Mølmer, *Phys. Rev. Lett.* 80 (1998) 1804.

[15] M. Amoruso, A. Minguzzi, S. Stringari, M.P. Tosi, L. Vichi, *Eur. Phys. J. D* 4 (1998) 261.

[16] N. Nygaard, K. Mølmer, *Phys. Rev. A* 59 (1999) 2974.

[17] M. Amoruso, C. Minniti, M.P. Tosi, *Eur. Phys. J. D* 8, (2000) 19.

[18] L. Vichi, M. Amoruso, A. Minguzzi, S. Stringari, M.P. Tosi, *cond-mat*/9909150 and Eur. Phys. J. D, in press.

[19] T. Miyakawa, T. Suzuki, H. Yabu, *cond-mat*/0002145.

[20] M. Amoruso, I. Meccoli, A. Minguzzi, M.P. Tosi, *Eur. Phys. J. D*, 8 (2000) 361.

[21] J.L. Bohn, J.P. Burke Jr., C.H. Greene, H. Wang, P.L. Gould and W.C. Stwalley, *Phys. Rev. A* 59 (1999) 3660.

[22] A. Minguzzi, M.L. Chiofalo, M.P. Tosi, *Phys. Lett. A* 236, (1997) 237.

[23] L. Viverit, C.J. Pethick, H. Smith, *cond-mat*/9911080.

[24] T. Miyakawa, T. Suzuki, H. Yabu, *cond-mat*/0002048.

[25] P. Ao, S.T. Chui, *Phys. Rev. A* 58 (1998) 4836.

[26] W. Kohn, *Phys. Rev.* 123 (1961) 1242.

[27] J. F. Dobson, *Phys. Rev. Lett.* 73 (1994) 2244.

[28] S. Stringari, *Phys. Rev. Lett.* 77 (1996) 2360.

[29] M. Amoruso, I. Meccoli, A. Minguzzi, M.P. Tosi, *Eur. Phys. J. D* 7 (1999) 441.

[30] M.R. Andrews, D.M. Kurn, H.-J. Miesner, D.S. Durfee, C.G. Townsend, S. Inouye, W. Ketterle, *Phys. Rev. Lett.* 79 (1997) 553 and 80 (1998) 2967.

[31] I.S. Gradshteyn, I.M. Ryzhik, "Tables of Integrals, Series and Products" (Academic Press, San Diego 1980).